ACS APPLIED MATERIALS & INTERFACES

Research Article

www.acsami.org

Synthesis of Semiconducting Polymer Microparticles as Solid Ionophore with Abundant Complexing Sites for Long-Life Pb(II) Sensors

Mei-Rong Huang,*[,†,‡] Yong-Bo Ding,[‡] Xin-Gui Li,*[,†,‡,§] YingJun Liu,[§] Kai Xi,[§] Chen-Long Gao,[§] and R. Vasant Kumar[§]

[†]State Key Laboratory of Pollution Control and Resource Reuse, College of Environmental Science and Engineering, Tongji University, Shanghai 200092, China

[‡]Key Laboratory of Advanced Civil Engineering Materials, College of Materials Science and Engineering, Tongji University, 1239 Si-Ping Road, Shanghai 200092, China

[§]Department of Materials Science and Metallurgy, University of Cambridge, Pembroke Street, Cambridge CB2 3QZ, United Kingdom

Supporting Information

ABSTRACT: Intrinsically electrically semiconducting microparticles of semiladder poly(*m*-phenylenediamine-*co*-2-hydroxy-5-sulfonic aniline) structures containing abundant functional groups, like —NH—, —N=, —NH_2, —OH, —SO_3H as complexation sites, were efficiently synthesized by chemical oxidative copolymerization of *m*-phenylenediamine and 2-hydroxy-5-sulfonic aniline. The obtained copolymers were found to be nonporous spherical microparticles that were able to achieve greater π-conjugated structure, smaller particle aggregate size, and stronger interaction with Pb(II) ions than poly(*m*-phenylenediamine) containing only —NH—, —N=, and —NH_2. A potentiometric Pb(II) sensor was fabricated on the basis of the copolymer microparticles as a crucial solid ionophore component within plasticized PVC. The sensor exhibited a Nernstian response to Pb(II) ions over a wide concentration range, together with a fast response, a wide pH range capability, a long lifetime of up to 5 months, and good selectivity over a wide variety of other ions and redox species. The process for synthesizing the microparticles and fabricating the Pb(II)-sensor can be facilely scaled-up for use in the straightforward long-term online monitoring of Pb(II) ions in heavily polluted wastewaters. This study develops an understanding of the facile synthesis of conducting microparticles bearing many functional groups and their structures governing the potentiometric susceptibility toward interaction between Pb(II) ions and the microparticles for fabricating robust long-lived Pb(II)-sensor, signifying the potential suitability of such novel materials for inexpensive sensitive detection of Pb(II) ions.

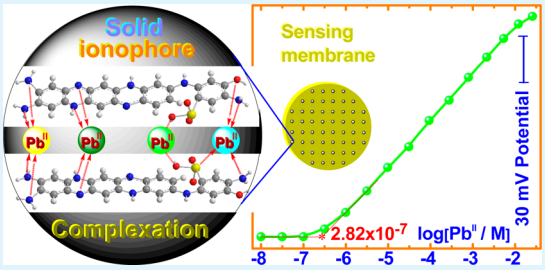

KEYWORDS: *sulfonic copolyaniline, semiconducting polymer, functional particle, solid lead ionophore, long-life Pb(II) sensor*

1. INTRODUCTION

During the past few decades there has been an increasing global concern over the public health impacts from environmental pollution. Lead(II) ions, among the most serious of environmental pollutants, have adverse effects as they accumulate in the body, especially for children and pregnant women, potentially resulting in behavior disorders, anemia, mental retardation, and permanent nerve damage. Therefore, it is very important to accurately measure the lead levels in the natural environment or in physiological fluids as early as possible. Universal detecting methods for trace lead are used, including atomic absorption spectrometry; inductively coupled plasma mass spectrometry;[1] and electrochemical,[2] colorimetric,[3,4] fluorometric,[5−9] and fluoro-chromogenic[10] sensing methods. The potentiometry, as one of the most important electroanalytical methods, is a direct method that does not require a pretreatment of samples and has apparent advantages including simple instrumentation, facile sensing membrane preparation, superior detection limit, fast response, wide dynamic range, high analyte selectivity, minimal use of toxic solvents, and low cost over most of the other methods. It is well-known that the ionophore is a crucial component embedded in the sensing membrane. It should ideally form relatively strong, selective, and reversible complexes only with the target ion, so that interference is absent.

One of the pioneering works exploring the possibility of improving the performance of Pb^{2+}-ISE by assembling the electrode technique is achieved.[11] They used ion buffered Pb^{2+} inner solution, achieved the lower detection limit of 3×10^{-9} M, and successfully assayed the heavy metal ion at nanomolar

Received: August 15, 2014
Accepted: November 18, 2014
Published: November 18, 2014

concentrations in drinking water. They also developed Au-POT-MMA/DMA solid-contact electrodes which showed better performance than the corresponding liquid-contact ISE, realizing a lower detection limit on subnanomolar level.[12] Some other excellent improvement on Pb^{2+}-ISE has been accomplished by developing polyarylates as sensing membrane matrix instead of plasticized PVC with the purpose of reducing the ion flux across sensing membrane, and furthermore introduced some Pt nanoparticles to enhance the conductivity of the membrane matrix.[13−15] Covalently binding the ionophore to polymer backbones is another promising solution that can efficiently help to reduce transmembrane ion fluxes.[16] The lower detection limit of 10^{-9} M could be reached by the Pb^{2+}-ISEs based on the ETH5234 (ionophore for lead ion) bonded to polyurethane using a conventional inner electrolyte (0.1 M $Pb(NO_3)_2$). Actually, solid ionophores were also developed for Ag^+-ISE, in which an ionophore-gold nanoparticle conjugate that confines the ionophore to ion-selective membranes using inert nanoparticle carriers is responsible for the nanomolar detection limit.[17] As inspired by this aforementioned work, other solid functional polymers, such as polyaminoanthraquinone,[18] sulfonic phenylenediamine copolymer,[19] and copolyaniline[20] synthesized in our group, have also been chosen for the design of the Pb^{2+}-ISE, and even better lower detection limit was achieved if combining plasticizer-free membrane with the solid ionophone. Despite these above advances, developing a simple, cost-effective ISE with superior lower detection limit and long lifetime that does not require sophisticated processing is still challenging.

Many ligands have been investigated as lead(II)-ISE ionophores incorporated into poly(vinyl chloride) membranes as matrix. The ionophores developed for the selective complexation or coordination of Pb(II) include macrocyclic compounds such as crown ethers,[21] calixarenes with right cavity size,[22] nitrogen compounds,[23] and some O/S atom-enriched organic compounds.[24] However, the above-mentioned ionophores generally require sophisticated synthesis conditions and tedious procedures, leading to difficulty in achieving wide practical application at low cost. One problem is the naturally insufficient stability of these ionophore-containing Pb(II) sensors due to inevitable loss of ionophores during usage process, consequently leading to short lifetime of the sensors. Recent studies suggested that some conjugated and/or electrically conducting polymers have significant interaction with metal ions,[20,25−30] such as copolyaniline and poly(*m*-phenylenediamine) (P*m*PD), when they were used as ionophore of Pb(II)-ISE,[20,31] where amino (—NH_2) and imino (—NH— and —N=) groups on and in the polymer chains play a key role in the complexation between the chains and the metal ions. Many functional-group-containing conducting polymers, such as carbon nanotubes, show extremely selective sensitivity toward changes in their local chemical environment that originates from the susceptibility of their electronic structure to trace amounts of specifically interacting molecules.[32] This chemical sensitivity has made them ideal candidates as ultrasensitive ionophores for incorporation into the design and fabrication of advanced sensors. It should be noted that the Pb(II)-sensor containing the P*m*PD homopolymer particles as ionophore does not seem to demonstrate very superior detection limit possibly due to their relatively poor particle dispersibility and also relatively fewer group species. It is reported that the aromatic amines bearing the sulfonic groups are an amazing copolymer modifier for significantly improving self-doping and stabilizing properties, heavy-metal ion interaction, and redispersibility of the corresponding particles. Developing new immobile leak proof polymer ionophores containing sulfonic and other functional groups on the polymer chains in order to (1) increase specific area of the particles and effect complexation interaction with the ions, (2) significantly lengthen the lifetime of the sensors, and (3) simplify synthetic process for producing these ionophores by a facilely scalable procedure remains a challenge.

In this Article, a new Pb(II) ionophore of semiladder poly(*m*-phenylenediamine-*co*-2-hydroxy-5-sulfonic aniline) microparticles containing five types of functional groups such as —NH_2, —NH—, —N=, —SO_3H, and —OH in/on the polymer chains was designed and synthesized by a direct chemical oxidative polymerization of *m*-phenylenediamine and 2-hydroxy-5-sulfonic aniline. The polymerization yield, molecular structure, supramolecular structure, particle size, morphology, and the resulting physical and chemical properties are discussed. Applications as ionophores for the fabrication of Pb(II)-sensor having relatively long lifetime have also been elaborated.

2. EXPERIMENTAL SECTION

2.1. Reagents. *m*-Phenylenediamine (*m*PD), 2-hydroxy-5-sulfonic aniline (HS), ammonium persulfate ($(NH_4)_2S_2O_8$), high molecular-mass poly(vinyl chloride) (PVC, dielectric constant 1.4), dioctyl phthalate (DOP, dielectric constant 5.1), tetrahydrofuran (THF), sodium tetraphenylborate (NaTPB), oleic acid (OA), lead nitrate ($Pb(NO_3)_2$), and other nitrates or chloride salts of cations as commercial reagents in analytical grade from China Chemicals Market are used as received. Working solutions with varying Pb(II) ion concentrations were produced by gradually diluting a 0.1 M $Pb(NO_3)_2$ stock solution. All sample solutions were prepared with highly pure water having electric resistance of higher than 18.0 MΩ cm.

2.2. Synthesis of Poly(*m*PD-*co*-HS) Microparticles. Poly(*m*PD-*co*-HS) copolymer particles as an ionophore were facilely prepared by a chemical oxidative copolymerization of *m*PD and HS comonomers, as illustrated in Scheme 1. A typical preparation procedure of the poly(*m*PD-*co*-HS) microparticles is as follows: *m*PD (2.055g, 19 mmol) and HS (0.211 g, 1 mmol) were mixed in a glass flask which contained 75 mL of 1.0 M HCl. Ammonium persulfate (4.564 g, 20 mmol) was dissolved separately in 25 mL of 1.0 M HCl to prepare an oxidant solution. Both of them were placed in a water bath at 30 °C for 30 min. The comonomer solution was then stirred and treated with the oxidant solution dropwise at a rate of one drop (60 μL) every 3 s over a period of 30 min at 30 °C. The reaction mixture was constantly magnetically stirred in the 30 °C water bath for 24 h, and then the resulting polymer microparticles were centrifuged and rinsed thoroughly with distilled water to entirely remove the residual oxidant, water-soluble oligomer, and other possible byproducts. The resulting black solid powders of as-prepared copolymer salts were left to dry in air at 50 °C for 3 days. The possible reaction formulation is displayed in Scheme 1.

2.3. Characterization of Poly(*m*PD-*co*-HS) Microparticles. UV−vis spectra were recorded by UV765CRT (Shanghai Jing-ke Instruments Factory, China). IR spectra were obtained by Nicolet FT-IR NEXUS-470 instrument. Raman spectra of the solid powder of the polymers and the polymer-based char were achieved by British Renishaw inVia Raman Microscope (Bert) by using laser at 785 nm solid state diode. X-ray photoelectron spectra were obtained by Kratos AXIS Ultra DLD instrument. Wide-angle X-ray diffractograms were recorded by Japan Rigaku D/max 2550 instrument. The size and morphology of the copolymer particles were observed by a Jeol JSM-6340F field emission scanning electron microscope (FE-SEM) and FEI Tecnai F20-G2 FEGTEM high-resolution transmission electron microscope (TEM). The samples for FE-SEM observation were dispersed by using ethanol on a silicon wafer and then subject to gold

Scheme 1. Nominal Chemical Oxidative Copolymerization of *m*-Phenylenediamine (*m*PD) and 2-Hydroxy-5-sulfonic Aniline (HS) for the Synthesis of the Semiladder or Partial Ladder Poly(*m*PD-*co*-HS) Microparticles Bearing Five Kinds of Functional Groups That Can Significantly Ligate Pb(II) Ions by Complexation (Green Dash Arrows) and Ion Exchange (Blue Dash Lines)

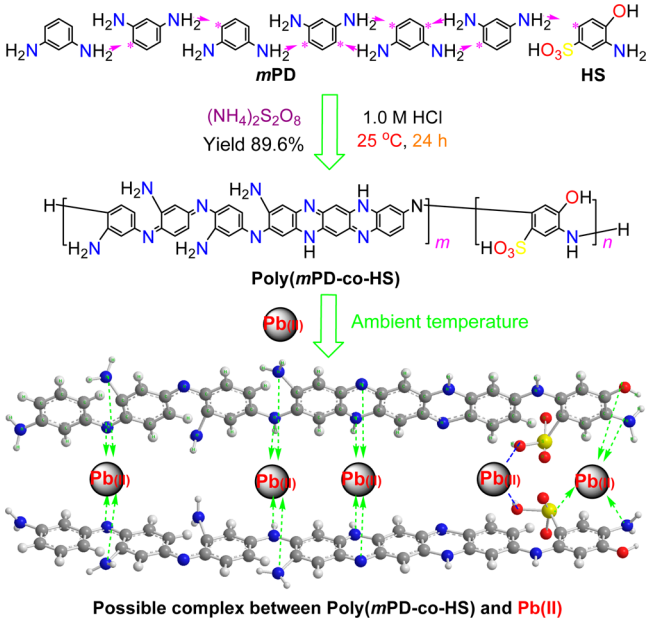

sputtering prior to observation. A dilute ethanol dispersion of the particle samples was ultrasonically prepared and dropped onto a copper grid covered with a carbon film to make a specimen for TEM observation. Particle size in water was analyzed by Beckman Coulter LS230 laser particle-size analyzer. The bulk electrical conductivity of the polymer particle sheet was obtained according to its thickness and resistance measured with a UNI-TUT70A multimeter.

2.4. Lead(II) Ion Adsorption onto the Microparticles. Adsorption of Pb^{2+} ions onto poly(*m*PD-*co*-HS) copolymer particles was performed by using batch experiments. For batch tests, a given amount of the copolymer microparticles was added to $Pb(NO_3)_2$ aqueous solution (10 mL) at a known concentration (0.965 mM) at a temperature of 30 °C. After a 30 min treatment, the microparticles were filtered from the aqueous solution. The concentration of lead ion in the filtrate after adsorption was measured by using chemical titrimetric analysis.[30] The amount of adsorbed lead ions on the microparticles was calculated according to eqs 1 and 2, where Q is the adsorption capacity (mg g^{-1}), q the adsorptivity (%), C_o and C the Pb(II) concentrations before and after adsorption (mg L^{-1}), respectively, V the initial volume of the Pb(II) solution (mL), and W the weight of the adsorbent added (mg).

$$Q = (C_o - C)V/W \quad (1)$$

$$q = (C_o - C)100\%/C_o \quad (2)$$

2.5. Preparation of Sensing Membrane and the Sensor Assembly. The procedure for preparing the PVC-based sensing membrane consisted of thoroughly mixing the ingredients of 183 mg of plasticizer DOP, 99 mg of high molecular-mass PVC, 3 mg of copolymer ionophore, and 15 mg of OA ion-exchanger in 5 mL of THF. The mixture was stirred at 25 °C to a viscous solution while ultrasonic treatment was also performed to promote the dissolution or dispersion of the ionophore for 2 h and then cast into a 28 mm diameter glass ring that was affixed onto a glass plate. After the solvent was allowed to evaporate at room temperature for 24 h, the resulting membranes were peeled off from the glass, and the membrane discs of 14 mm diameter were cut out and carefully glued onto a 10 mm inner diameter plastic tube. A 1.0×10^{-4} M $Pb(NO_3)_2$ solution was used as an inner reference system, and Ag/AgCl electrode was employed as an inner reference electrode. The electrodes were conditioned in 1.0×10^{-4} M $Pb(NO_3)_2$ solution overnight.

2.6. Potential Measurement. All response potentials were precisely examined by using the following electrochemical assembly setup:

$$\mathrm{Ag|AgCl|KCl(saturated\ solution)||\ Pb(NO_3)_2(1.00 \times 10^{-4}\ M)}$$

$$\mathrm{|PVC\ sensing\ membrane|test\ solution\ ||\ KNO_3(1.00\ M)}$$

$$\mathrm{||\ KCl(saturated\ solution)|Hg_2Cl_2|Hg}$$

Saturated calomel electrode (SCE) was applied as an outer reference electrode, and the cell potential was measured by varying the concentration of test solutions in a range between 1.00×10^{-8} and 1.00×10^{-1} M. Potentials were measured with PXSJ-216 potentiometer (Shanghai Lei-Ci Instruments Factory, China) with a sensitivity of 0.1 mV and an input resistance of greater than 1×10^{12} Ω. The potential readings were recorded after the response potential remained stable (drift < 1 mV/5 min). The potential response curves were plotted as a logarithmic function of Pb(II) ionic activity. The activities of the primary ions were based on the activity coefficient, which is calculated according to Debye−Huckel equation:

$$\log r_i = -0.509 Z_i^2 \frac{I^{0.5}}{1 + BaI^{0.5}} \quad (3)$$

Here I is the total ionic strength of the tested solution, Z_i the valency of Pb(II) ions, B constant of 0.328 $Å^{-1}$ at 25 °C, and a volume coefficient of Pb(II), which is approximately equal to effective radius of Pb(II) (5 Å).

The response time of the electrode was determined by measuring the time which elapsed between the instant when the ISE and a reference electrode were brought into contact at which the activity of the lead(II) ions in the solution was changed and the first instant at which the emf/time slope ($\Delta E/\Delta t$) became equal to 0.6 mV/min. The lower detection limit was taken as the activity of Pb(II) ions at the point of intersection of the extrapolated linear midrange and final low concentration level segments of the calibration plot. Selectivity characteristics were determined according to the IUPAC recommended fixed interference method. All pH adjustments were made with HNO_3 or NaOH solution.

2.7. Lifetime Measurement. The lifetime of the Pb(II)-sensor was measured by the following process: after the sensor was fabricated, the detection performance to Pb(II) was recorded about twice a week in the first month. During daily use, the electrode was stored in a 1.00×10^{-4} M $Pb(NO_3)_2$ solution. After the ISE had been used for a month, its performance including Nernstian slope and linear range was measured again once every week. If the slope was above 95% of the first test slope, we considered that the sensor to be alive, otherwise rejected as out of its lifetime.

3. RESULTS AND DISCUSSION

3.1. Synthesis of the Copolymer Microparticles. The chemical oxidative copolymerization of *m*PD and HS monomers with ammonium persulfate as an oxidant in 1.0 M HCl aqueous solution at 30 °C produces fine and uniform black microparticles as a resultant product with a semiladder or partial ladder chain structure,[30,31,33,34] as illustrated in Scheme 1. Figure 1 shows that the polymerization yield increases monotonically from 26.0% to 91.6% with increasing *m*PD content from 0% to 100%. That is to say, more *m*PD monomers would steadily strengthen the polymerization activity, resulting in higher synthetic yield. It is obvious that the synthesis of poly(*m*PD-*co*-HS) microparticles is efficient or productive when the *m*PD monomer ratio is higher than 90 wt % or HS ratio is less than 10 wt %. On the contrary, more HS monomers would weaken the polymerization activity because

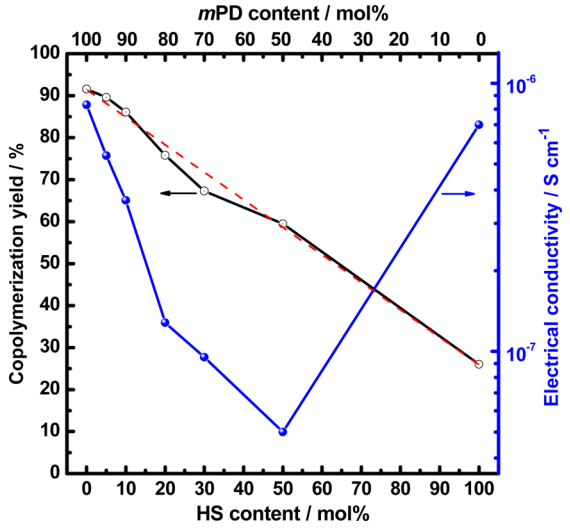

Figure 1. Variation of copolymerization yield and electrical conductivity of the copolymer particles with *m*PD/HS molar ratio at the initial polymerization temperature of 30 °C for 24 h. The red dashed line means a simple addition of two homopolymer yields.

of stronger and stronger steric hindrance, attracting electron effect, and water-soluble tendency from sulfonic groups in HS monomer. Note that HS monomer and its homopolymer are water-soluble, and the HS homopolymer can be obtained only when a nonaqueous precipitator like acetone is used instead of water, but all other six polymer samples with *m*PD and HS molar ratios from 100/0 to 50/50 have been purified or washed with water. However, the copolymerization between *m*PD and HS actually happens because the electrical conductivity of the polymers nonmonotonically changes with HS contents, i.e., decreases first and then increases, giving a minimum conductivity of 5.03×10^{-8} S/cm at an HS content of 50 mol %, because the sulfonic and hydroxyl groups introduced into *m*PD units can induce torsion in the copolymer backbones, thereby shortening the conjugation length.[35−38] However, HS homopolymer demonstrates slightly lower conductivity than *m*PD homopolymer but much higher conductivity than *m*PD/HS(50/50) copolymer, possibly due to higher chain structure regularity and thus better self-doping effect than the copolymers.

Furthermore, the *m*PD/HS (50/50) copolymerization can semiquantitatively be confirmed by the yield of up to 59.5% that is higher than 50%. At least 9.5 mol % HS units have been incorporated into the polymer chains, forming copolymer chains. Otherwise, all HS homopolymer should be washed away from the final products by water. Assuming that copolymerization follows a simple addition of two homopolymer yields of 91.6 and 26.0 for *m*PD and HS comonomers, respectively, as predicted by the red dash line in Figure 1, the copolymerization yield would be 58.8%. However, higher actual yield of 59.5% implies that copolymerization does happen between *m*PD and HS comonomers. The polymerization at other comonomer ratios from 70/30 to 80/20 is a slightly negative copolymerization effect but a positive copolymerization effect at the comonomer ratios from 90/10 to 95/5.

3. 2. Macromolecular and Supramolecular Structure of Copolymer Microparticles. *UV−Vis Spectra.* UV−vis absorption spectra of the copolymer salts in DMSO in Figure 2a show four characteristic bands: the strongest band 1 around 265−285 nm due to $\pi-\pi^*$ transition of all aromatic rings in copolymer chains, which has a blue shift compared with the aniline/sulfonic aniline copolymer;[37] the weak band 3 in a long wavelength range of 550−650 nm due to $n-\pi^*$ excitation of benzenoid to the quinoid ring in the polymer chains; the

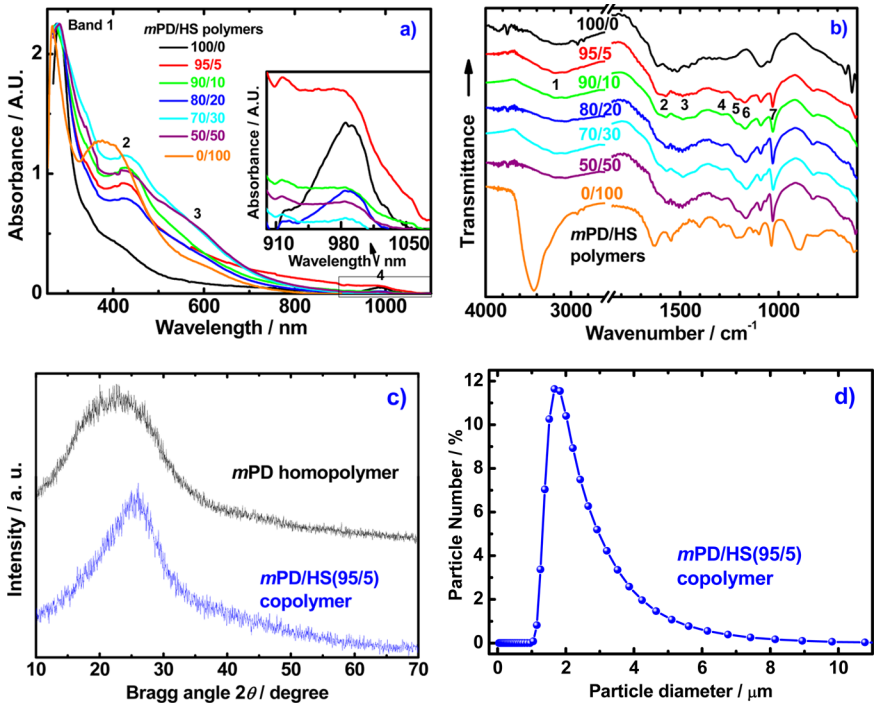

Figure 2. (a) UV−vis in DMSO and (b) FT-IR spectra of the copolymer particles with seven *m*PD/HS molar ratios. (c) Wide-angle X-ray diffractograms and (d) the size distribution of the polymer microparticles of *m*PD/HS molar ratios of 100/0 and 95/5 synthesized with $(NH_4)_2S_2O_8$/monomer molar ratio of 1/1 in 1.0 M HCl at 30 °C.

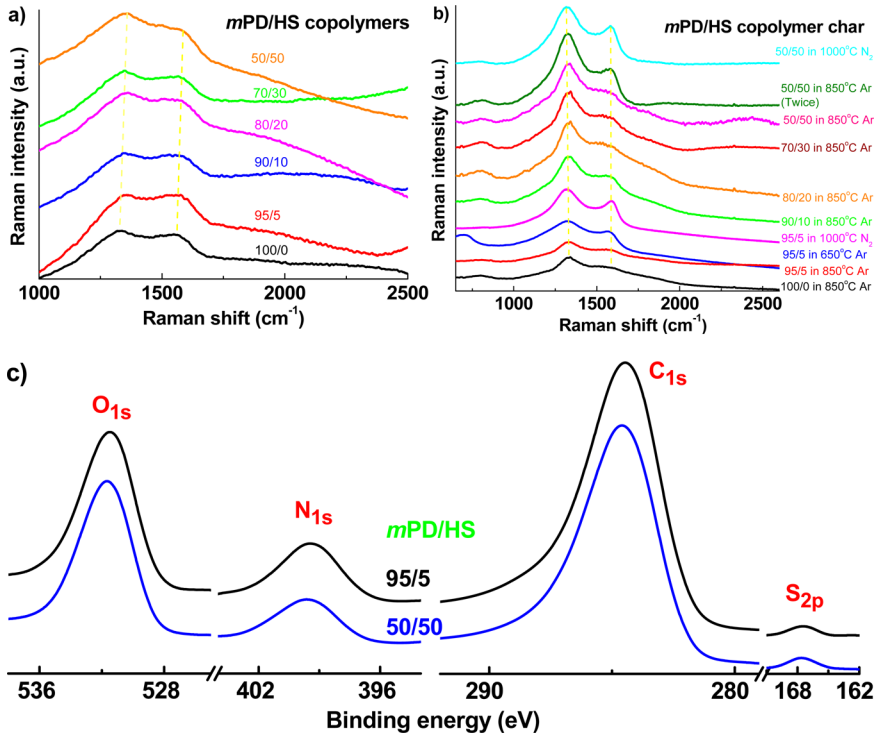

Figure 3. Raman spectra of (a) the copolymer particles with six *m*PD/HS molar ratios and (b) the copolymer particle-based char at high temperature in two inert atmospheres (argon and nitrogen) and (c) the X-ray photoelectron spectra (XPS) of two typical copolymer microparticles of *m*PD/HS molar ratios of 95/5 and 50/50 synthesized with $(NH_4)_2S_2O_8$/monomer molar ratio of 1/1 in 1.0 M HCl at 30 °C.

medium band 2 at 370−450 nm mainly due to HS units in the copolymers because only a very weak band 2 appears in the *m*PD homopolymer,[30] an indication of the existence of the HS units in the synthesized copolymer; the weakest band 4 at 910−1090 nm mainly due to *m*PD units in the copolymers because stronger band 4 appears in the polymers containing more *m*PD units. Note that the *m*PD/HS(95/5) copolymer has stronger band 4 than the *m*PD homopolymer, and the *m*PD/HS(50/50) copolymer also has stronger band 4 than the *m*PD/HS(70/30) copolymer, because the *m*PD homopolymer generally has lower solubility in DMSO than the *m*PD/HS(95/5) copolymer containing a small amount of HS units that can improve the solubility in common solvents. In fact, only the lower molecular-weight part in the *m*PD homopolymer could be soluble in DMSO, leading to weaker band 4 than the *m*PD/HS(95/5) copolymer. Considering that, the *m*PD/HS(50/50) copolymer has higher solubility in aqueous HCl medium than the *m*PD/HS(70/30) copolymer containing a lower amount of HS units. That is, during the post purification process, some *m*PD/HS(50/50) copolymer containing less than 50 mol % *m*PD units would be acidic water-soluble and then removed, leading to lower synthetic yield and higher *m*PD-unit content than 50% or even 70% in the final water-insoluble copolymer obtained. However, the situation about band 2 is more complicated since the band 2 may be related to both the small π-conjugation inside the phenylene rings and the large π-conjugation along the polymer chains. Therefore, it is hard to explain the complicated relationship between the band 2 intensity and *m*PD/HS ratio.

There is no significant absorption in the UV−vis spectra of both monomers at a wavelength of longer than 350 nm,[30,35] possibly indicating that a copolymerization indeed occurred between *m*PD and HS comonomers. Moreover, all five copolymers exhibit stronger band 3 in a wavelength range from 500 to 900 nm than two homopolymers, and particularly *m*PD/HS(95/5) copolymer always has the strongest absorption in a wavelength range from 700 to 1090 nm. These two facts would suggest that the copolymers possessing more π-conjugated structure are achieved, which could be used to verify a positive copolymerization effect mentioned earlier.

IR Spectra. Figure 2b shows the IR spectra of the microparticles of seven representative polymers. The broad and weak bands 1 at 3188 and 3313 cm^{-1} correspond to the N−H stretching of amine, imine, and/or O−H stretching.[30,35] The *m*PD/HS(95/5) copolymer demonstrates that the stronger band at 3100−3300 cm^{-1} could be the evidence that there are more N−H and O−H groups in the copolymer than two homopolymers. The two absorptions specified as 2 and 3 at 1611 and 1489 cm^{-1} are associated with the stretching of quinoid and benzenoid rings,[37,38] respectively. It is revealed that there are more benzenoid rings in the *m*PD unit-containing copolymer shown in Scheme 1 than HS homopolymer, but the *m*PD/HS(95/5) copolymer is an exception. The weak absorption peak 4 of C−N vibration in *m*PD units lies at 1289 cm^{-1}, which coincides with an earlier analysis.[39] The stronger bands 5 and 6 at 1214 and 1176 cm^{-1}, respectively, are associated with the C−N stretching on the HS units because HS homopolymer also has two similar strong absorption,[35] but the *m*PD homopolymer does not. The sharpest absorption band 7 at 1031 cm^{-1} may be related to the symmetric stretching vibration of the $-SO_3^-$ group on the HS units. In short, these adsorption bands evidently indicate that the products obtained are not the mixture of the two homopolymers but indeed true copolymers, because water-soluble HS homopolymers have been removed completely.

Raman Spectra. Figure 3a shows the Raman spectra of the solid microparticles of six representative polymers. Two characteristic Raman absorbance bands centered at 1328 and 1563 cm^{-1} correspond to the Raman vibration of C−N and quinoid/benzenoid rings, respectively. It is found that both of the bands gradually shift to higher wavenumber, and these peak shifts are evidence for copolymer formation one more time, because the polymer-based char at 650−850 °C in argon and 1000 °C in nitrogen demonstrated almost constant Raman shifts at 1318 and 1587 cm^{-1} due to D- and G-bands, respectively, regardless of the *m*PD/HS ratio variation, as shown in Figure 3(b).

X-ray Photoelectron Spectra (XPS). Figure 3c shows the XPS spectra of the microparticles of two representative copolymer microparticles of *m*PD/HS molar ratios of 95/5 and 50/50. The symmetry of the S_{2p} peaks is very good, signifying only one type of S atom in sulfonic groups. The symmetry of the N_{1s} and O_{1s} peaks is not as good as the S_{2p} peaks but still good, since there are three types of N and O atoms, respectively, in —NH—/—N=/—NH_2 and O═S/HO—S/HO—C groups. The asymmetry of the C_{1s} peak is the highest, which is the evidence that five types of C atoms in C—N, C—H, C═N, C—S, and C—O groups all exist in the copolymers. These XPS spectra have been used to calculate the atomic composition of C, N, O, and S in the copolymers, as listed in Table 1. It is seen that observed C content in the two

Table 1. Atomic Composition for Two Typical *m*PD/HS Copolymers

*m*PD/HS (mol/mol)	C_{1s} (wt %)	N_{1s} (wt %)	O_{1s} (wt %)	S_{2p} (wt %)
95/5 (exptl)	75.1	8.3	15.1	1.5
95/5 (theoretical)	70.3	27.0	1.8	0.9
50/50 (exptl)	75.6	6.6	16.0	1.8
50/50 (theoretical)	51.1	14.9	22.7	11.36

samples is higher than theoretical one, while the *m*PD/HS(95/5) copolymer has higher experimental O and S content than theoretical ones, because more than 5 mol % HS monomers could participate in the copolymerization that results in the copolymers containing more than 5 mol % HS units. However, less than 50 mol % HS monomers could participate in the *m*PD/HS(50/50) copolymerization that produces the *m*PD/HS(50/50) copolymers containing less than 50 mol % HS units, in which the experimental N, O, and S content is lower than theoretical content. These results are in agreement with the above relevant discussion.

Wide-Angle X-ray Diffractograms. The wide-angle X-ray diffractograms of the microparticles of the *m*PD/HS(95/5) copolymer and *m*PD homopolymer in Figure 2c present broad diffraction peaks in a Bragg angle range from 15° to 35°, which is typical diffraction of amorphous polymers. Hence two polymer microparticles have amorphous structure characteristics. It seems that the *m*PD homopolymer has even higher amorphous level. This amorphous structure should favor the penetration, interaction, and then adsorption of heavy metal ions into the microparticles because the macromolecular chains in the amorphous states are relatively looser and more disordered than those in the crystalline states.

3.3. Size and Morphology of Poly(*m*PD-*co*-HS) Microparticles. Particle size is one of the most important factors that influence the interaction degree between the particles and heavy metal ions. Smaller size usually indicates higher specific surface area and more active acting sites exposed on the surface for otherwise similar nonporous polymer particles. Considering that the *m*PD/HS (95/5) copolymer particles have the second highest synthetic yield, the third-highest conductivity, the highest band 4 intensity of UV−vis spectra, and the strongest interaction with Pb(II) ions (as shown later), the size distribution and morphology of the *m*PD/HS (95/5) copolymer particles have been carefully analyzed, as revealed in Figures 2d and 4. The number-average diameter of the

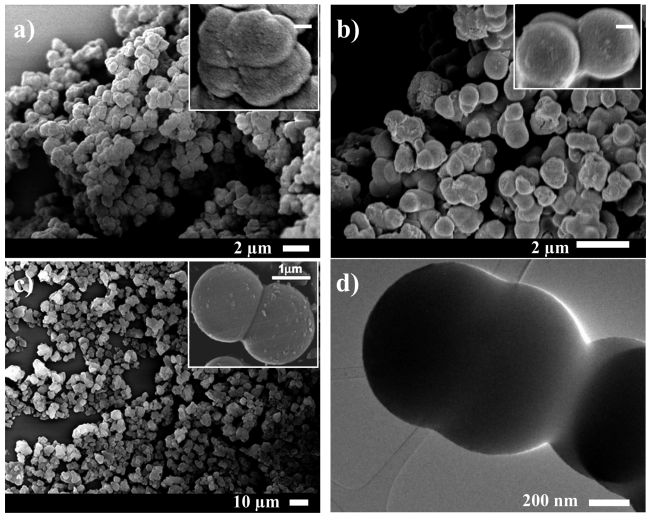

Figure 4. SEM and TEM images of *m*PD/HS (a) 100/0, (b) 95/5, (c, d) 70/30 copolymer microparticles synthesized under $(NH_4)_2S_2O_8$/comonomer molar ratio of 1/1 in 1.0 M HCl at 30 °C.

copolymer particles is found to be 2.44 μm that is smaller than that of the *m*PD homopolymer (3.16 μm).[30] The decrease of the particle size in water media should be attributed to improved water-dispersibility of the copolymer particles because of electrostatic repulsion of the negatively charged sulfonic and also hydroxyl groups on HS units,[35,36] which could efficiently stabilize the small particles with high surface energy. Note that the size polydispersity index of the copolymer particles is 2.16 that is slightly higher than that of the *m*PD homopolymer (1.17), signifying that the copolymer particles are basically uniform fine particles. Thus, smaller fine particles would result in more efficient interaction between the *m*PD/HS (95/5) copolymer and Pb(II) ions.

Since the copolymer particles could agglomerate to some extent in water, the size of the particles given by laser particle-size analysis is larger than that by SEM and TEM sometimes. SEM observation in Figure 4 indicates that all of the *m*PD/HS copolymer particles also aggregate into large particles to some extent regardless of ethanol dispersion. However, some particles dispersed well and have an average diameter of down to around 500, 700, 900, 1600, 2000, and 1100 nm for the *m*PD/HS copolymer particles of 100/0, 95/5, 90/10, 80/20, 70/30, and 50/50, respectively. It seems that the elementary particles of the *m*PD/HS(100/0) polymer, i.e., *m*PD homopolymer, are the smallest, but their dispersion is the weakest. It is of interest to find that the *m*PD/HS(95/5) copolymer particles have the second smallest size and the best dispersion. The field-emission TEM images in Figure 4d further confirmed that the *m*PD/HS(95/5) copolymer microparticles are smaller than *m*PD/HS(70/30) copolymer microparticles, having average diameters of 600 and 800 nm, respectively.

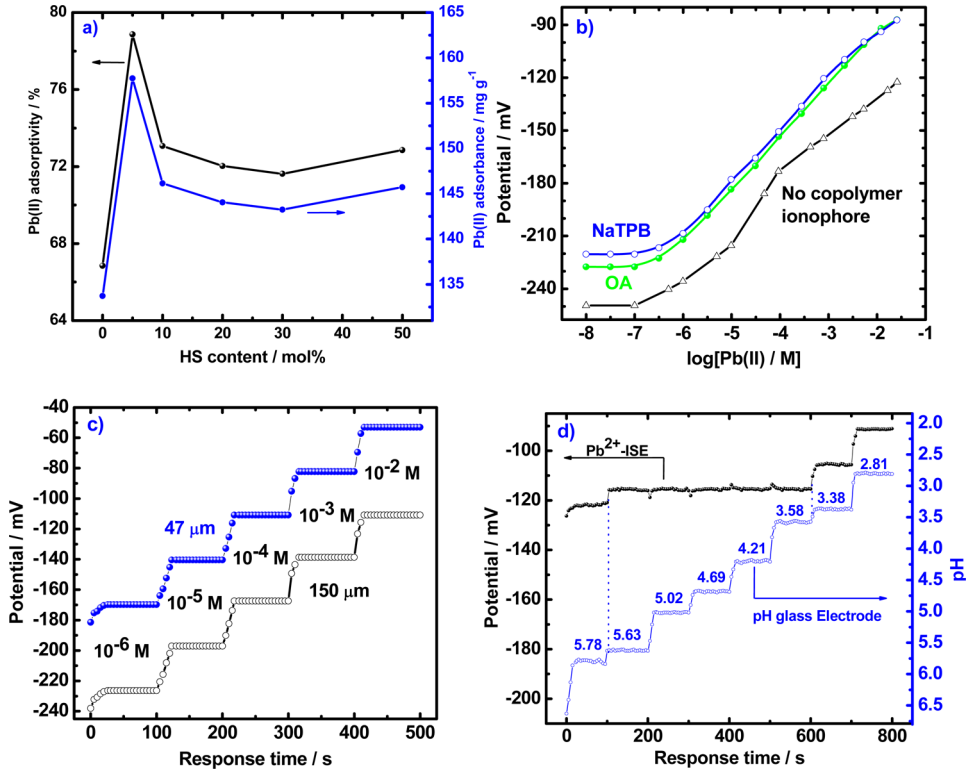

Figure 5. (a) Adsorption of Pb(II) at an initial Pb(II) concentration of 0.965 mM onto *m*PD/HS copolymer particles with a sorbent dose of 10 mg at 30 °C for 0.5 h. (b) Potentiometric response of Pb(II) sensor based on *m*PD/HS copolymer:PVC:DOP (1.0:33.0:61.0) sensing membrane with a thickness of 150 μm with two ion-exchangers of OA and NaTPB. (c) Dynamic response time profiles of the Pb(II) sensors with *m*PD/HS copolymer:PVC:DOP:OA ratio of 1.0:33.0:61.0:5.0 in two membrane thicknesses of 150 and 47 μm. (d) Effect of pH on the response potential at Pb(II) concentrations of 1.0×10^{-3} M with *m*PD/HS copolymer:PVC:DOP:OA ratio of 1.0:33.0:61.0:5.0.

Moreover, the copolymer is a kind of loose aggregate consisting of spherical nonporous particles. This morphological feature of the *m*PD/HS copolymer particles is propitious to the significant interaction or complexation between the copolymer chains and lead(II) ions when using the copolymer particles as a crucial ionophore in Pb(II) sensors.

3.4. Pb(II) Sensor Based on Poly(*m*PD-*co*-HS) Ionophore. *Complexation of Poly(mPD-co-HS) with Lead Ions.* One of the important interactions between the poly(*m*PD-*co*-HS) particles and Pb(II) ions is complexation of Pb(II) ions onto the ligating functional groups like —NH—, —N=, —OH, —SO_3H, and —NH_2 on the copolymer.[31] The complexation could quantitatively be described by adsorption capacity and adsorptivity of Pb(II) onto the microparticles as shown in Figure 5a. The adsorption capability is heavily dependent on the polymer composition. As the HS content increases from 0 to 50 mol %, the adsorbance and adsorptivity both significantly rise first and then decrease, simultaneously demonstrating the maximal adsorbance and adsorptivity of 157.74 mg g^{-1} and 78.87%, respectively, at the HS content of 5 mol %. Compared to the *m*PD homopolymer particles, the *m*PD/HS (95/5) copolymer particles have an adsorptivity enhancement by 12.02%, which can be ascribed to the introduction of an optimal amount of ligating active sulfonic and hydroxyl groups and the best dispersion of the particles in Pb(II) aqueous solution as shown in Figure 4b. That is to say, the interaction between the *m*PD/HS (95/5) copolymer and Pb(II) ions could be the strongest. Therefore, this specific copolymer particles have been used as novel ionophore for the fabrication of Pb(II) sensor in the following investigation.

Sensing Performance of Pb(II) Sensors. As can be seen in Figure 5b, both the potentiometric sensors with poly(*m*PD-*co*-HS) particles as an ionophore show satisfactory Nernstian response to Pb(II) ions over a wide range, especially for the sensor with 5 wt % OA as ion exchanger. In other words, a lipophilic OA additive would result in a wider linear range than hydrophilic tetraphenylborate salt. The detection limit and linear range of the former sensor are found to be $10^{-6.55}$ M and $10^{-6.5}$–$10^{-1.9}$ M, respectively, which are superior to $10^{-6.38}$ M and $10^{-6.0}$–$10^{-2.3}$ M of the latter. Superior detection sensitivity to Pb(II) may be attributable to a unique synergistic complexation effect between —NH_2/—NH—/—N=/—OH/—SO_3H groups and Pb(II) ions. The superiority of OA may result from fewer hydrogen ions from OA (pK_a = 5.02), which would be helpful to realize lower detection limit.[40] It should be noticed that a copolymer particles-free electrode with copolymer:PVC:DOP:OA weight ratio of 0:33:61:5.0 showed the poorest linear potential response simply because of the absence of copolymer sensing materials that can achieve the valuable complexation between the copolymer ionophore and Pb(II) ions. That is to say, 1 wt % of the copolymer particles in the sensing membranes plays a vital role in linear and sensitive response to Pb(II) ions. The linear sensitive response might be attributable to a unique ability for tendency of the particles to connect with each other and accordingly form a nanochannel or nanonetwork of effectively conducting electrons and ions over the entire sensing membrane.[37] Therefore, OA was selected as the ion-exchanger for the following sensor study.

The response time of the sensor to Pb(II) ions is mainly determined by the interaction rate between Pb(II) ions and the

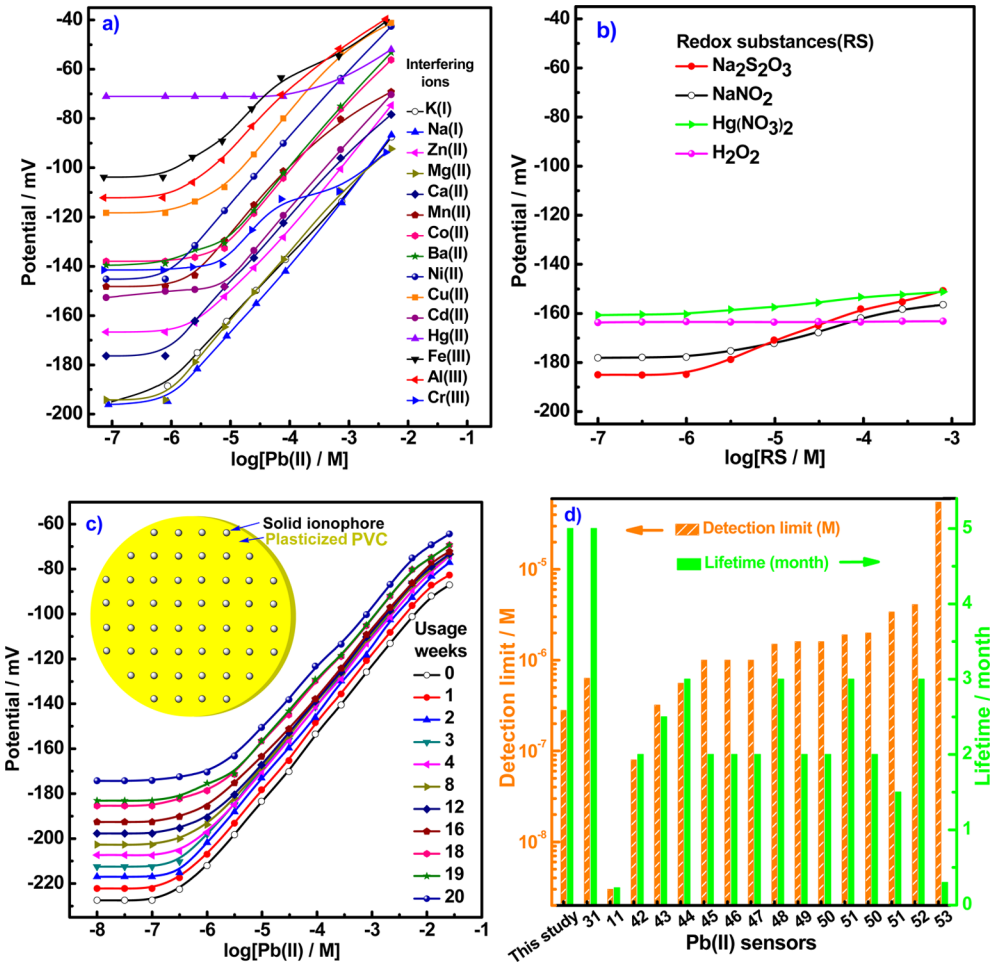

Figure 6. (a) Potential response curves of the Pb(II)-sensors by fixed interference method at an interfering ion concentration of 1.00×10^{-3} M. (b) Potential response curves of the Pb(II)-sensors (conditioned and inner filled with 1.0×10^{-4} M $Pb(NO_3)_2$) toward respective four redox species solutions in the same concentration range from 1.0×10^{-7} to $1.0 \times 10^{-3.1}$ M. (c) Potential response curves of Pb(II)-sensors based on membrane with a thickness of ca. 150 μm filling with inner solution of 1.0×10^{-4} M $Pb(NO_3)_2$ with usage time. Inset: Schematized sensing membranes containing solid semiconducting copolymer microparticles as ionophore in plasticized PVC. (d) Comparison of detection limit and lifetime of Pb(II)-sensors in plasticized PVC based on *m*PD/HS(95/5) copolymer ionophore and other 16 types of representative ionophores mainly having potential response slope of 28.8 to 29.8 in the literature.[11,31,42−53]

Table 2. Logarithmic Selectivity Coefficients for the Pb(II)-Sensors by a Fixed Interference Method at an Interfering Ion Concentration of 1.00×10^{-3} M[a]

compound	interfering ion	detection limit (M)	selectivity coeff $K^{pot}_{Pb,B}$	logarithmic selectivity coeff log $K^{pot}_{Pb,B}$
$NaNO_3$	Na(I)	$10^{-6.1}$	$10^{-6.1}/(10^{-3})^{2} = 10^{-0.1}$	−0.1
KNO_3	K(I)	$10^{-6.3}$	$10^{-6.3}/(10^{-3})^{2} = 10^{-0.3}$	−0.3
$Hg(NO_3)_2$	Hg(II)	$10^{-3.5}$	$10^{-3.5}/10^{-3} = 10^{-0.5}$	−0.5
$Co(NO_3)_2$	Co(II)	$10^{-5.3}$	$10^{-5.3}/10^{-3} = 10^{-2.3}$	−2.3
$CdCl_2$	Cd(II)	$10^{-5.3}$	$10^{-5.3}/10^{-3} = 10^{-2.3}$	−2.3
$Ba(NO_3)_2$	Ba(II)	$10^{-5.4}$	$10^{-5.4}/10^{-3} = 10^{-2.4}$	−2.4
$Cu(NO_3)_2$	Cu(II)	$10^{-5.4}$	$10^{-5.4}/10^{-3} = 10^{-2.4}$	−2.4
$Zn(NO_3)_2$	Zn(II)	$10^{-5.6}$	$10^{-5.6}/10^{-3} = 10^{-2.6}$	−2.6
$Mn(NO_3)_2$	Mn(II)	$10^{-5.8}$	$10^{-5.8}/10^{-3} = 10^{-2.8}$	−2.8
$Ca(NO_3)_2$	Ca(II)	$10^{-6.1}$	$10^{-6.1}/10^{-3} = 10^{-3.1}$	−3.1
$Mg(NO_3)_2$	Mg(II)	$10^{-6.1}$	$10^{-6.1}/10^{-3} = 10^{-3.1}$	−3.1
$Ni(NO_3)_2$	Ni(II)	$10^{-6.2}$	$10^{-6.2}/10^{-3} = 10^{-3.2}$	−3.2
$Cr(NO_3)_3$	Cr(III)	$10^{-5.2}$	$10^{-5.2}/(10^{-3})^{2/3} = 10^{-3.2}$	−3.2
$AlCl_3$	Al(III)	$10^{-5.7}$	$10^{-5.7}/(10^{-3})^{2/3} = 10^{-3.7}$	−3.7
$FeCl_3$	Fe(III)	$10^{-5.7}$	$10^{-5.7}/(10^{-3})^{2/3} = 10^{-3.7}$	−3.7

[a]The standard deviations for the triplicate tests are between 0.58 and 0.82.

Table 3. Characteristics of Pb(II) Ion-Sensors Based on *m*PD/HS Copolymer Ionophores with a Thickness of ca. 150 μm Filling with Inner Solution of 1.00×10^{-4} M $Pb(NO_3)_2$ with Usage Time[a]

usage time (week)	linear range (M)	fitting eq	linear correlation coeff	slope (mV/decade)	detection limit (M)
0	$10^{-6.5}$–$10^{-1.9}$	$E = -35.72 + 29.28 \log a$	0.9994	29.28	$10^{-6.55} = 2.82 \times 10^{-7}$
1	$10^{-6.5}$–$10^{-1.9}$	$E = -30.93 + 29.23 \log a$	0.9994	29.23	$10^{-6.54} = 2.88 \times 10^{-7}$
2	$10^{-6.5}$–$10^{-1.9}$	$E = -26.77 + 29.20 \log a$	0.9997	29.20	$10^{-6.51} = 3.09 \times 10^{-7}$
3	$10^{-6.5}$–$10^{-1.9}$	$E = -22.77 + 29.18 \log a$	0.9994	29.18	$10^{-6.50} = 3.16 \times 10^{-7}$
4	$10^{-6.0}$–$10^{-1.9}$	$E = -29.32 + 29.04 \log a$	0.9997	29.04	$10^{-6.30} = 5.01 \times 10^{-7}$
8	$10^{-6.0}$–$10^{-1.9}$	$E = -23.30 + 28.76 \log a$	0.9995	28.76	$10^{-6.24} = 5.75 \times 10^{-7}$
12	$10^{-6.0}$–$10^{-1.9}$	$E = -23.49 + 28.38 \log a$	0.9991	28.38	$10^{-6.14} = 7.24 \times 10^{-7}$
16	$10^{-5.5}$–$10^{-1.9}$	$E = -23.10 + 28.05 \log a$	0.9993	28.05	$10^{-6.04}$=9.12 $\times 10^{-7}$
18	$10^{-5.5}$–$10^{-2.3}$	$E = -17.94 + 27.91 \log a$	0.9995	27.91	$10^{-6.00} = 1.00 \times 10^{-6}$
19	$10^{-5.5}$–$10^{-2.3}$	$E = -17.78 + 27.84 \log a$	0.9996	27.84	$10^{-5.94} = 1.15 \times 10^{-6}$
20	$10^{-5.5}$–$10^{-2.3}$	$E = -14.99 + 27.11 \log a$	0.9992	27.11	$10^{-5.88} = 1.32 \times 10^{-6}$

[a]The standard deviations for the triplicate tests range from 0.58 to 0.82.

ligating groups on copolymer particles. To measure the response time of the proposed Pb(II)-ISE, the Pb(II) concentration of the test solution was successively changed from $1.0 \times 10^{-6.0}$ to $1.0 \times 10^{-2.0}$ M. Figure 5c shows that the dynamic response time of the Pb(II)-sensor decreased from 25 to 16 s with increasing Pb(II) concentration from $1.0 \times 10^{-6.0}$ to $1.0 \times 10^{-2.0}$ M. Very similar response rate for the Pb(II)-sensors containing two membrane thicknesses of 150 and 47 μm suggests that the crucial potentiometric sensing interaction mainly occurred at the skin layer of the sensing membranes rather than the bulk layer. The fast response at high Pb(II) concentration is probably due to the fast exchange kinetics of complexation−decomplexation of Pb(II) at the interface between Pb(II) solution and sensing membrane.

A study on the potential−pH relationship of Pb(II) sensor based on poly(*m*PD-*co*-HS) solid ionophores reveals that, in a pH range between 3.58 and 5.63 (Figure 5d), the potential is quite stable with pH. That is, the Pb(II) sensor could be satisfactorily used in the pH range from 3.58 to 5.63. At pH > 5.63, the potential decreased related either to precipitation of $Pb(OH)_2$ and/or to formation of hydroxyl lead complexes resulting from competition of OH^- with the ionophores for Pb(II) ions.[41] The carbonate complexation may also form in this case.[11] Contrarily, the potential variation at pH < 3.58 could be related to protonation of the ligands in the membrane phase and ion-exchanger OA can release H^+ to the sample solution near the membrane side, which resulted in a loss of its ability to form complexes with Pb(II) ions.

The sensing selectivity is obviously one of the most important characteristics of an ion-sensor, determining whether a reliable measurement in the target sample is possible. The selectivity coefficient was determined by the fixed interference method (FIM) on the basis of the potential of the solutions containing a fixed amount of the interfering ions (B^+) (1.0×10^{-3} M) and varying amounts of Pb(II) ions. As can be seen from Figure 6a and Table 2, with the exception of Hg(II), for all other divalent or trivalent interfering ions used, the selectivity coefficients of cations tested are smaller than 5.0×10^{-3}, which seems to indicate that these metal ions exert negligible disturbances on the functioning of the Pb(II) membrane sensor. As far as the most common monovalent interfering ions are concerned, the logarithmic selectivity coefficients range from −0.1 to −0.3, signifying that small interference is present. However, it must be noted that a direct comparison of the numerical values of the selectivity coefficients would be insignificant for the interfering ions with different charges. In fact, interferences are comparable for the Pb(II)-ISE in the presence of 1.00×10^{-3} M monovalent or divalent interfering ions with logarithmic selectivity coefficients of 1 or −2, respectively.[31] Considering that Na(I) and Hg(II) could be possible interfering ions, the potential response of the Pb(II) sensor with *m*PD/HS copolymer:PVC:DOP:OA ratio of 1.0:33.0:61.0:5.0 toward four representative redox species ($Na_2S_2O_3$, $NaNO_2$, $Hg(NO_3)_2$, and H_2O_2) present in solutions in a wide concentration range from 1.0×10^{-7} to $1.0 \times 10^{-3.1}$ M has been reported in Figure 6b. It is found that $Na_2S_2O_3$ slightly contributes to potential response slope. However, $NaNO_2$, $Hg(NO_3)_2$, and H_2O_2 hardly ever contribute to potential response slope; i.e., the coexistence of $NaNO_2$, $Hg(NO_3)_2$, and H_2O_2 will not disturb the potential response of the sensors toward Pb(II). Therefore, the Pb(II)-sensor revealed comparatively good selectivity with respect to many cations including alkali earth, alkaline earth, transition and heavy metal ions, and ordinary redox species such as $NaNO_2$, Hg(II) and H_2O_2.

The copolymer ionophore synthesized in this study contains abundant functional groups like —NH—, —N=, —NH_2, —OH, —SO_3H as complexation sites. These groups possess lone pair electrons that are readily attracted by the metal ions with electron deficiency. The selectivity originates from the differences of the electron deficiency of the metal ions. In fact, the functional groups employed have very low binding capability toward the alkaline and alkaline earth metal ions, and also low binding capability toward most of the transition metal ions except Pb(II), Hg(II), Fe(III), and Al(III) with deficient electrons. This proper binding capability should result from the formation of the charge-transfer complex between the functional groups and Pb(II)/Hg(II)/Fe(III)/Al(III) ions. Theoretically, the potential response of trivalent Fe(III) and Al(III) is weaker than those from divalent or monovalent ions at the same complexation extent because of the much weaker theoretical Nernstian response slopes from trivalent ions, resulting in much lower interfering effect of the trivalent ions on Pb(II) response even if the same quantity of ions are complexed. It seems that there should be an interference from Hg(II) to some extent. However, Hg(II) concentration in the real environmental world is generally low. Therefore, in most circumstances, the interference from Hg(II) to the detection of Pb(II) would be avoided.

Long-term inspection for the Pb(II)-sensor showed a long lifetime as listed in Table 3. In a period of 4 weeks' usage at a frequency of twice a week, the proposed sensor still retained

good performance, and then continued at the same level for over 20 weeks (5 months) without any divergence in potentials but just with a small shift in the detection limit, as shown in Figure 6c. The sensor has such a long lifetime because the solid copolymer ionophore used in this investigation will not leak during long-term usage regardless of a possible loss of the liquid plasticizer. Another reason could be that the water-insoluble OA has been used to totally replace partly water-soluble NaTPB. It might be concluded that the optimal *m*PD/HS copolymer:PVC:DOP:OA weight ratio in the sensing membrane as schematized in Figure 6c, inset, for long-lived Pb sensor is 1.0:33.0:61.0:5.0 for fabricating a robust long-life Pb(II)-sensor.

Comparative Benefits. The synthetic process of the *m*PD/HS(95/5) copolymer particles having synthetic yield of up to 89.6% is simpler and more efficient and could be more scalable than that of other ionophores. The *m*PD/HS(95/5) copolymer incorporating ca. 5 mol % —OH/—SO_3H groups to replace a small amount of —NH_2 groups demonstrates 2.25 times better detection limit than the *m*PD homopolymer without —OH/—SO_3H groups,[31] which would be attributed to the effectively synergistic effect among —NH_2, —NH—, —N=, —OH, and —SO_3H groups while ligating Pb(II) ions. This synergistic effect hardly ever exists in the complexation reaction between Pb(II) and *m*PD homopolymer. In a comparison with other typical Pb(II)-ISE sensors with plasticized PVC as matrix,[11,31,42−53] the proposed Pb(II)-sensor with the copolymer ionophore having five types of different functional groups that could appropriately ligate Pb(II) ions along the unique large π-conjugated macromolecular chains, and intrinsic electrical conductivity accomplishes superior comprehensive performance including longer lifetime time (green bar) and/or the third best detection limit (orange bar), as summarized in Figure 6d and Supporting Information Table S1. As compared with the previous article,[20] the shortest response time of the new sensor to Pb(II) where *m*PD and DOP-plasticized PVC were used instead of aniline and plasticizer-free vinyl resin is improved from 22 to 16 s. The higher electric conductivity of the DOP-plasticized sensing membrane in this study than in the plasticizer-free vinyl resin membrane[20] also significantly results in a more facile and time-saving measurement of the potential. It seems that these two types of Pb(II) sensors have different characteristics and thus different application fields. The previous sensor could be suitable for the Pb(II) analysis of the pure water containing an extremely trace amount of Pb(II), while the current sensor should be suitable for the Pb(II) analysis of the wastewater containing relatively more Pb(II) ions.

In short, the conducting copolymer microparticles demonstrate sensitive, selective, quick, and long-term detection of a trace amount of aqueous Pb(II) ions in a pH range between 3.58 and 5.63 because of their highly potentiometric sensitivity toward Pb(II) concentration changes that stems from the linear and quantitative susceptibility of their electronic structure to interacting Pb(II) ions. This potentiometric sensitivity makes the copolymer particles become an ideal ultrasensitive ionophore in PVC membrane matrix in order to fabricate Pb(II)-sensors for sensitively and selectively determining Pb(II) ions at low cost.

4. CONCLUSIONS

A new *m*PD/HS copolymer possessing five types of different functional groups that may properly ligate Pb(II) ions along the unique large π-conjugated macromolecular chains and intrinsic electrical conductivity has been successfully synthesized as spherical and nonporous microparticles. The conducting copolymer microparticles demonstrate ultrasensitivity toward changes in their local chemical environment that stems from the linear and quantitative susceptibility of their electronic structure to interacting Pb(II) ions. This chemical sensitivity has made them an ideal ultrasensitive ionophore in PVC membrane matrix for fabrication of Pb(II)-sensors for sensitively and selectively determining Pb(II) at potentially much lower cost and simpler sensing membrane preparation procedure than the present PVC-based Pb(II)-sensors containing low molecules as ionophores. This is demonstrated by good performance characteristics obtained during application, such as low concentration detection limit, short response time, wide pH windows, long lifetime, and good selectivity. In particular, the new long-life Pb sensors based on a novel sensing membrane with many complexation sites and thus fast and stable response have been achieved by a simplified process. The process for producing the copolymer microparticles and fabricating Pb(II)-sensor can be easily scaled-up in order to supply robust sensors for facile use in the relatively long-term online monitoring of Pb(II) in real world applications such as heavily polluted wastewaters when even more highly sensitive Pb(II) sensors could not be directly applicable.

■ ASSOCIATED CONTENT

Supporting Information

Systematic comparison of Pb(II) ion-sensors in plasticized PVC based on *m*PD/HS(95/5) copolymer ionophore and other ionophores mainly having slope 28.8−29.8 in the literature. This material is available free of charge via the Internet at http://pubs.acs.org.

■ AUTHOR INFORMATION

Corresponding Authors

*E-mail: adamxgli@yahoo.com.
*E-mail: huangmeirong@tongji.edu.cn.

Notes

The authors declare no competing financial interest.

■ ACKNOWLEDGMENTS

The project is supported by the National Natural Science Foundation of China (51273148). Y.J.L. and K.X. acknowledge the support from UK-India Education and Research Initiative and the Cambridge Overseas Trust, respectively. We would like to thank Mr. Kristofer L. Marsh and Prof. R. B. Kaner in the Department of Chemistry, UCLA, for their XPS measurement and analysis.

■ REFERENCES

(1) Yilmaz, V.; Arslan, Z.; Rose, L. Determination of Lead by Hydride Generation Inductively Coupled Plasma Mass Spectrometry (HG-ICP-MS): On-Line Generation of Plumbane Using Potassium Hexacyanomanganate(III). *Anal. Chim. Acta* **2013**, *761*, 18−26.

(2) Xiao, Y.; Rowe, A. A.; Plaxco, K. W. Electrochemical Detection of Parts-per-Billion Lead via an Electrode-Bound DNAzyme Assembly. *J. Am. Chem. Soc.* **2007**, *129*, 262−263.

(3) Liu, J. W.; Lu, Y. Accelerated Color Change of Gold Nanoparticles Assembled by DNAzymes for Simple and Fast Colorimetric Pb^{2+} Detection. *J. Am. Chem. Soc.* **2004**, *126*, 12298−12305.

(4) Wang, Z.; Lee, J. H.; Lu, Y. Label-Free Colorimetric Detection of Lead Ions with a Nanomolar Detection Limit and Tunable Dynamic Range by using Gold Nanoparticles and DNAzyme. *Adv. Mater.* **2008**, *20*, 3263−3267.
(5) Deo, S.; Godwin, H. A. A Selective, Ratiometric Fluorescent Sensor for Pb^{2+}. *J. Am. Chem. Soc.* **2000**, *122*, 174−175.
(6) He, Q. W.; Miller, E. W.; Wong, A. P.; Chang, C. J. A Selective Fluorescent Sensor for Detecting Lead in Living Cells. *J. Am. Chem. Soc.* **2006**, *128*, 9316−9317.
(7) Huang, Y.; Li, F. Y.; Qin, M.; Jiang, L.; Song, Y. L. A Multi-Stopband Photonic-Crystal Microchip for High-Performance Metal-Ion Recognition Based on Fluorescent Detection. *Angew. Chem., Int. Ed.* **2013**, *52*, 7296−7299.
(8) Schäferling, M. The Art of Fluorescence Imaging with Chemical Sensors. *Angew. Chem., Int. Ed.* **2012**, *51*, 3532−3554.
(9) Marbella, L.; Serli-Mitasev, B.; Basu, P. Development of A Fluorescent Pb^{2+} Sensor. *Angew. Chem., Int. Ed.* **2009**, *48*, 3996−3998.
(10) Son, H.; Lee, H. Y.; Lim, J. M.; Kang, D.; Han, W. S.; Lee, S. S.; Jung, J. H. A Highly Sensitive and Selective Turn-On Fluorogenic and Chromogenic Sensor Based on BODIPY-Functionalized Magnetic Nanoparticles for Detecting Lead in Living Cells. *Chem.—Eur. J.* **2010**, *16*, 11549−11553.
(11) Ceresa, A.; Bakker, E.; Hattendorf, B.; Gunther, D.; Pretsch, E. Potentiometric Polymeric Membrane Electrodes for Measurement of Environmental Samples at Trace Levels: New Requirements for Selectivities and Measuring Protocols, and Comparison with ICPMS. *Anal. Chem.* **2001**, *73*, 343−351.
(12) Sutter, J.; Radu, A.; Peper, S.; Bakker, E.; Pretsch, E. Solid-Contact Polymeric Membrane Electrodes with Detection Limits in the Subnanomolar Range. *Anal. Chim. Acta* **2004**, *523*, 53−59.
(13) Michalska, A.; Pyrzynska, K.; Maksymiuk, K. Method of Achieving Desired Potentiometric Responses of Polyacrylate-Based Ion-Selective Membranes. *Anal. Chem.* **2008**, *80*, 3921−3924.
(14) Lyczewska, M.; Kakietek, M.; Maksymiuk, K.; Mieczkowski, J.; Michalska, A. Comparison of Trihexadecylalkylammonium Iodides as Ion-Exchangers for Polyacrylate and Poly(vinyl chloride) Based Iodide-selective Electrodes. *Sens. Actuators, B* **2010**, *146*, 283−288.
(15) Jaworska, E.; Kisiel, A.; Maksymiuk, K.; Michalska, A. Lowering the Resistivity of Polyacrylate Ion-Selective Membranes by Platinum Nanoparticles Addition. *Anal. Chem.* **2011**, *83*, 438−445.
(16) Püntener, M.; Vigassy, T.; Baier, E.; Ceresa, A.; Pretsch, E. Improving the Lower Detection Limit of Potentiometric Sensors by Covalently Binding the Ionophore to a Polymer Backbone. *Anal. Chim. Acta* **2004**, *503*, 187−194.
(17) Jágerszki, G.; Alajos, G. A.; Bitter, I.; Tóth, K.; Gyurcsányi, R. E. Ionophore-Gold Nanoparticle Conjugates for Ag+-Selective Sensors with Nanomolar Detection Limit. *Chem. Commun.* **2010**, *46*, 607−609.
(18) Li, X. G.; Ma, X. L.; Huang, M. R. Lead(II) Ion-Selective Electrode Based on Polyaminoanthraquinone Particles with Intrinsic Conductivity. *Talanta* **2009**, *78*, 498−505.
(19) Huang, M. R.; Ding, Y. B.; Li, X. G. Lead-Ion Potentiometric Sensor Based on Electrically Conducting Microparticles of Sulfonic Phenylenediamine Copolymer. *Analyst* **2013**, *138*, 3820−3829.
(20) Li, X. G.; Feng, H.; Huang, M. R.; Gu, G. L.; Moloney, M. G. Ultrasensitive Pb (II) Potentiometric Sensor Based on Copolyaniline Nanoparticles in A Plasticizer-free Membrane with A Long Lifetime. *Anal. Chem.* **2012**, *84*, 134−140.
(21) Sheen, S. R.; Shih, J. S. Lead(II) Ion-Selective Electrodes Based on Crown Ethers. *Analyst* **1992**, *117*, 1691−1695.
(22) Guziński, M.; Lisak, G.; Sokalski, T.; Bobacka, J.; Ivaska, A.; Bocheńska, M.; Lewenstam, A. Solid-Contact Ion-Selective Electrodes with Highly Selective Thioamide Derivatives of p-tert-Butylcalix[4]-arene for the Determination of Lead(II) in Environmental Samples. *Anal. Chem.* **2013**, *85*, 1555−1561.
(23) Ion, I.; Culetu, A.; Costa, J.; Luca, C.; Ion, A. C. Polyvinyl Chloride-Based Membranes of 3,7,11-Tris (2-pyridylmethyl)-3,7,11,17-tetraazabicyclo [11.3.1] Heptadeca-1(17),13,15-triene as A Pb(II)-Selective Sensor. *Desalination* **2010**, *259*, 38−43.
(24) Faridbod, F.; Ganjali, M. R.; Larijani, B.; Hosseini, M.; Alizadeh, K.; Norouzi, P. Highly Selective and Sensitive Asymmetric Lead Microsensor Based on 5,5-Dithiobis(2-nitrobenzoic acid) as an Excellent Hydrophobic Neutral Carrier for Nano Level Monitoring of Lead in Real Samples. *Int. J. Electrochem. Soc.* **2009**, *4*, 1528−1540.
(25) Liang, J.; Li, K.; Liu, B. Visual Sensing with Conjugated Polyelectrolytes. *Chem. Sci.* **2013**, *4*, 1377−1394.
(26) Li, X. G.; Liao, Y. Z.; Huang, M. R.; Strong, V.; Kaner, R. B. Ultra-Sensitive Chemosensors for Fe (III) and Explosives Based on Highly Fluorescent Oligofluoranthene. *Chem. Sci.* **2013**, *4*, 1970−1978.
(27) Thomas, S. W.; Joly, G. D.; Swager, T. M. Chemical Sensors Based on Amplifying Fluorescent Conjugated Polymers. *Chem. Rev.* **2007**, *107*, 1339−1386.
(28) McQuade, D. T.; Pullen, A. E.; Swager, T. M. Conjugated Polymer-Based Chemical Sensors. *Chem. Rev.* **2000**, *100*, 2537−2574.
(29) Zeng, Q.; Cai, P.; Li, Z.; Qin, J.; Tang, B. Z. An Imidazole-Functionalized Polyacetylene: Convenient Synthesis and Selective Chemosensor for Metal Ions and Cyanide. *Chem. Commun.* **2008**, *9*, 1094−1096.
(30) Huang, M. R.; Lu, H. J.; Li, X. G. Synthesis and Strong Heavy-Metal Ion Sorption of Copolymer Microparticles from Phenylenediamine and Its Sulfonate. *J. Mater. Chem.* **2012**, *22*, 17685−17699.
(31) Huang, M. R.; Rao, X. W.; Li, X. G.; Ding, Y. B. Lead Ion-Selective Electrodes Based on Polyphenylenediamine as Unique Solid Ionophores. *Talanta* **2011**, *85*, 1575−1584.
(32) Kauffman, D. R.; Star, A. Carbon Nanotube Gas and Vapor Sensors. *Angew. Chem., Int. Ed.* **2008**, *47*, 6550−6570.
(33) Li, X. G.; Duan, W.; Huang, M. R.; Yang, Y. L. Preparation and Characterization of Soluble Terpolymers from *m*-Phenylenediamine, *o*-Anisidine, and 2,3-Xylidine. *J. Polym. Sci., Part A: Polym. Chem.* **2001**, *39*, 3989−4000.
(34) Li, X. G.; Duan, W.; Huang, M. R.; Yang, Y. L.; Zhao, D. Y.; Dong, Q. Z. A Soluble Ladder Copolymer from *m*-Phenylenediamine and Ethoxyaniline. *Polymer* **2003**, *44*, 5579−5595.
(35) Li, X. G.; Hou, Z. Z.; Huang, M. R.; Moloney, M. G. Efficient Synthesis of Intrinsically Conducting Polypyrrole Nanoparticles Containing Hydroxy Sulfoaniline as Key Self-Stabilized Units. *J. Phys. Chem. C* **2009**, *113*, 21586−21595.
(36) Li, X. G.; Lü, Q. F.; Huang, M. R. Self-Stabilized Nanoparticles of Intrinsically Conducting Copolymers from 5-Sulfonic-2-anisidine. *Small* **2008**, *4*, 1201−1209.
(37) Lü, Q. F.; Huang, M. R.; Li, X. G. Synthesis and Heavy-Metal-Ion Sorption of Pure Sulfophenylenediamine Copolymer Nanoparticles with Intrinsic Conductivity and Stability. *Chem.—Eur. J.* **2007**, *13*, 6009−6018.
(38) Li, X. G.; Lü, Q. F.; Huang, M. R. Facile Synthesis and Optimization of Conductive Copolymer Nanoparticles and Nanocomposite Films from Aniline with Sulfodiphenylamine. *Chem.—Eur. J.* **2006**, *12*, 1349−1359.
(39) Li, X. G.; Huang, M. R.; Duan, W.; Yang, Y. L. Novel Multifunctional Polymers from Aromatic Diamines by Oxidative Polymerizations. *Chem. Rev.* **2002**, *102*, 2925−3030.
(40) Arvand, M.; Asadollahzadeh, S. A. Ion-Selective Electrode for Aluminum Determination in Pharmaceutical Substances, Tea Leaves and Water Samples. *Talanta* **2008**, *75*, 1046−1054.
(41) Perera, W. N.; Hefter, G.; Sipos, P. M. An Investigation of the Lead(II)−Hydroxide System. *Inorg. Chem.* **2001**, *40*, 3974−3978.
(42) Mazloum-Ardakani, M.; Safari, J.; Pourhakkak, P.; Sheikh-Mohseni, M. A. Determination of Lead (II) Ion by Highly Selective and Sensitive Lead (II) Membrane Electrode Based on 2-(((E)-2-((E)-1- (2-hydroxyphenyl)methyliden)hydrazono)metyl)phenol. *Int. J. Environ. Anal. Chem.* **2012**, *92*, 1638−1649.
(43) Abbaspour, A.; Mirahmadi, E.; Khalafi-nejad, A.; Babamohammadi, S. A Highly Selective and Sensitive Disposable Carbon Composite PVC-based Membrane for Determination of Lead Ion in Environmental Samples. *J. Hazard. Mater.* **2010**, *174*, 656−661.
(44) Zamani, A. A.; Khorsihdi, N.; Mofidi, Z.; Yaftian, M. R. Crown Ethers Bearing 18C6 Unit; Sensory Molecules for Fabricating PVC

Membrane Lead Ion-selective Electrodes. *J. Chin. Chem. Soc. (Taipei, Taiwan)* **2011**, *58*, 673−680.
(45) Rizk, N. M. H.; Abbas, S. S.; Hamza, S. M.; El-Karem, Y. M. A. Thiopental and Phenytoin as Novel Ionophores for Potentiometric Determination of Lead (II) Ions. *Sensors* **2009**, *9*, 1860−1875.
(46) Yan, Z. N.; Dan, J. Y.; Li, L. Q.; Wang, S. Q.; Zhao, B. T. Lead (II) Ion-Selective Membrane Electrodes Based on Four Nitrogen-Containing Heterocyclic Thioethers. *Sens. Lett.* **2012**, *10*, 43−51.
(47) Rouhollahi, A.; Ganjali, M. R.; Shamsipur, M. Lead Ion Selective PVC Membrane Electrode Based on 5, 5′-Dithiobis-(2-nitrobenzoic acid). *Talanta* **1998**, *46*, 1341−1346.
(48) Yan, Z. N.; Zhang, Q.; Dan, J. Y.; Guo, Y. P.; Li, L. Q. Lead(II) and Copper(II) Ion-Selective Electrodes Based on Two Heterocyclic Compounds. *J. Anal. Chem.* **2011**, *66*, 974−980.
(49) Wilson, D.; Arada, M. D.; Alegret, S.; del Valle, M. Lead(II) Ion Selective Electrodes with PVC Membranes Based on Two Bis-thioureas as Ionophores: 1,3-Bis(N′-benzoylthioureido)benzene and 1,3-Bis(N′-furoylthioureido)benzene. *J. Hazard. Mater.* **2010**, *181*, 140−146.
(50) Kazemi, S. Y.; Shamsipur, M.; Sharghi, H. Lead-Selective Poly(vinyl chloride) Electrodes Based on Some Synthesized Benzo-Substituted Macrocyclic Diamides. *J. Hazard. Mater.* **2009**, *172*, 68−73.
(51) Elsalamouny, A. R.; Elreefy, S. A.; Hassan, A. M. A. Lead Ion Selective Electrode Based on 1, 5-Diphenylthiocarbazone. *Res. J. Chem. Sci.* **2012**, *2*, 38−42.
(52) Lutfullah, M.; Rashid, N. Rahman, Potentiometric Sensor for the Determination of Lead(II) Ion Based on Zirconium(IV) Iodosulpho-salicylate. *Sci. Adv. Mater.* **2012**, *4*, 1232−1237.
(53) Hajiaghababaei, L.; Kazemi, S.; Badiei, A.; Zarabadi-Poor, P.; Ganjali, M. R.; Ziarani, G. M. Using the Hydroxymethyl-Modified Nanoporous Silica as a PVC Membrane Electrode Modifier to Determination of Lead Ions. *Anal. Bioanal. Electrochem.* **2012**, *4*, 246−261.